Available online at www.sciencedirect.com

ScienceDirect

Procedia CIRP 66 (2017) 210 – 214

www.elsevier.com/locate/procedia

1st Cirp Conference on Composite Materials Parts Manufacturing, cirp-ccmpm2017

Analysis and Modeling of Heat Flux into the Tool in Abrasive Circular Cutting of Unidirectional CFRP

Wolfgang Hintze[a]*, Christian Klingelhöller[b]

[a]*Institute of Production Management and Technology (IPMT), Hamburg University of Technology (TUHH), Germany*
[b]*ModuleWorks GmbH, Aachen, Germany*

* Corresponding author. Tel.: +49-40-42878-3051; fax: +49-40-42878-22 95. *E-mail address:* w.hintze@tuhh.de

Abstract

For edge trimming of slightly curved thin walled CFRP parts dry circular cutting is a promising alternative. However, a high fraction of the cutting energy is converted into heat. The study focuses on the determination of the amount of heat dissipated by the tool in circular cutting of unidirectional CFRP with epoxy matrix. An inverse heat conduction model is developed and solved for a set of temperature profiles measured on the tool surface with an infrared camera. It was found, how the heat dissipation by the diamond abrasive cut-off wheel is affected by fiber orientation, cutting speed, feed velocity and immersion depth of the wheel. The projected cutting area normal to the fiber direction turned out to be crucial for heat dissipation. The results of numerical simulations and experiments indicate, that tool temperatures in dry circular cutting do not exceed temperature limits of CFRP present in dry end milling. The developed heat flux model allows for optimization of dry CFRP abrasive circular cutting processes. It forms a module for future workpiece temperature assessment and thermo-mechanical process simulation.

Peer-review under responsibility of the scientific committee of the 1st Cirp Conference on Composite Materials Parts Manufacturing

Keywords: Temperature; Composite; Modeling; Grinding

1. Introduction

Carbon fiber reinforced plastics (CFRP) are increasingly used for light weight structures in several branches. However, production cost of CFRP structures is still a serious obstacle for a wider application. Because near net shape technologies available for CFRP do not yet fulfil precision requirements of most CFRP components their edges and holes need to be machined after consolidation. The developed length of edges of individual CFRP parts may amount to some meters in automotive and up to some hundred meters in aeronautic industry. CFRP shell components are mostly characterized by small wall thickness and predominantly by slight curvature of their surface and edges.

Edge trimming of CFRP parts is commonly done in full width cut by end milling, by cut-off grinding with a circular saw or a grinding point, by abrasive water jet, rarely by laser cutting [1, 2, 3, 4]. Regarding end milling tools and grinding points feed velocity is limited and tool wear increases rapidly even when using diamond cutting materials [5, 3, 6]. This implies high tool cost and risk of process-induced part damaging, particularly in dry machining. Abrasive circular cutting wheels seem beneficial with regard to heat dissipation and feed velocity but are restricted to straight contours. Abrasive water jet machining is often favorable as long as only edges need to be trimmed. Nevertheless, in case of narrow cut-outs, precision holes and counterbores machining technologies are indispensable [7, 6].

Thus, dry abrasive circular cutting is expected to be a promising alternative for edge trimming overcoming the above mentioned limitations and drawbacks provided that not only straight but also slightly curved edges can be machined. Fundamentals of suitable rigid or flexible grinding tools and according process kinematics for curved circular cutting have been published recently [8, 9]. However, dry grinding of CFRP requires careful control of heat generation and optimum heat dissipation by the tool in order to avoid thermal degradation of machined components. Hence, this study focuses on analysis of heat flux into the tool in abrasive circular cutting of unidirectional CFRP.

Peer-review under responsibility of the scientific committee of the 1st Cirp Conference on Composite Materials Parts Manufacturing
doi:10.1016/j.procir.2017.03.305

Several authors investigated heat flux and temperatures in dry CFRP machining by experimental and analytical methods [6, 10, 11, 12, 13, 14, 15, 16, 17]. Surface temperatures of unidirectional CFRP specimens and ratio of heat flux into specimen were determined in plunge grinding combining measurements with thermocouple and FEM simulations [14]. Results indicate increase of heat flux ratio into the specimen with lower cutting and higher feed velocities. If the grinding velocity is directed longitudinal to the fiber axis heat flux ratio and temperature increase of the specimen are slightly higher than in case of transversally directed grinding velocity. Similar results were found in surface grinding by experiments and FDM simulation [10]. Dry surface grinding of quasi-isotropic CFRP laminate using a vitrified aluminum oxide grinding wheel leads to progressive growth of work piece temperature with decreasing distance to the machined surface with a maximum of 376°C [15]. These measured temperatures result in particular from the low heat conductivity of the aluminum oxide wheel [18].

Also in dry end milling of CFRP maximum temperatures in the cutting zone easily reach more than 300°C up to 500°C exceeding the glass transition temperature of the resin which is in the range of 130°C to 180°C for epoxy [6, 13].

Whereas surface grinding of CFRP is carried out at low depth of cut $a_e < 0.2$ mm, in cut-off grinding with an abrasive circular cutting wheel a_e equals the material thickness t of several millimeters. In addition, tool width is preferably small. Hence, heat dissipation to the front face of the trimmed component needs to be considered [5].

2. Modeling of heat flux in abrasive circular cutting

Since experimental evaluation of heat flux into the work piece and access to the maximum local temperature in the cut-off grinding zone are difficult, these quantities are derived from measured tool temperature distributions and grinding force Fc / power consumption $P_c = v_c F_c$ together with a model of heat exchange. Prior to that, the model is established and its thermal parameters $\mathbf{p} = [p_1,\ldots,p_s]^T$ are fitted to the measured data. These parameters specify the amplitude and shape of the input heat flux, the heat conductivity of the tool λ and the heat transfer coefficient tool to air α.

Power consumption P_c during dry abrasive circular cutting is assumed to be totally converted into heat. In the cutting zone heat flux splits to tool, work piece and chips:

$$P_c = \left(P_{\text{workpiece}} + P_{\text{chip}}\right) + P_{\text{tool}} = (1-\eta)P_c + \eta P_c \tag{1}$$

The coefficient η representing heat flux fraction into the tool is unknown. Thus, the term ηP_c represents a boundary condition for the model, which will be identified together with other model parameters **p** by solving the according inverse heat conduction problem (IHCP).

2.1. Solving the inverse heat conduction problem

IHCP allows for parameter estimation of mathematical models based on their output quantities [19]. Here, parameter vector **p** of the direct heat flux model of the tool needs to be identified such that the squared error between simulated and measured temperature fields of the tool face side $\mathbf{T}_l^k$ and $\mathbf{Y}_l^k$ are minimized [20]:

$$S(\mathbf{p}) = \sum_{l=0}^{o}\sum_{k=0}^{t}\left(\mathbf{Y}_l^k - \mathbf{T}_l^k(\mathbf{p})\right)^2 \rightarrow \min \tag{2}$$

To solve the problem the Levenberg-Marquardt algorithm is applied, where $\mathbf{\Psi}^q$ designates an additional diagonal matrix and μ^q a damping parameter [21].

$$\mathbf{p}^{q+1} = \mathbf{p}^q + \left[\left(\mathbf{J}^q\right)^T\mathbf{J}^q + \mu^q\mathbf{\Psi}^q\right]^{-1}\left(\mathbf{J}^q\right)^T\left[\mathbf{Y} - \mathbf{T}(\mathbf{p}^q)\right]$$
$$\text{with } \mathbf{J} = \left[\frac{\partial\mathbf{T}^T(\mathbf{p})}{\partial\mathbf{p}}\right]^T \tag{3, 4}$$

2.2. Basic equations for the numerical simulation of direct heat flux

According to Fourier's law the heat flux density in a rigid body is proportional to the thermal conductivity λ and the vector **T** of temperature gradients normal to the isothermal surface.

Calculation of temperature change of a solid control volume caused by the heat flux density leads to the general heat equation which can be expressed in cylinder coordinates [22]:

$$\frac{1}{r}\frac{\partial}{\partial r}\left(\lambda r\frac{\partial\mathbf{T}}{\partial r}\right) + \frac{1}{r^2}\frac{\partial}{\partial\phi}\left(\lambda\frac{\partial\mathbf{T}}{\partial\phi}\right) + \frac{\partial}{\partial z}\left(\lambda\frac{\partial\mathbf{T}}{\partial z}\right) = \rho c_p\frac{\partial\mathbf{T}}{\partial t} \tag{5}$$

Whereas ρ is the density and c_p the specific heat capacity of the solid. This set of equations is approximated by means of the finite difference method (FDM). Therefore, using only the first terms of a Taylor series the derivatives are expressed by difference equations:

$$\mathbf{T}(t^k + \delta t) = \mathbf{T}(t^k) + \delta t\left.\frac{\partial\mathbf{T}}{\partial t}\right|_{\mathbf{T}(t^k)} + \frac{\delta t^2}{2}\left.\frac{\partial^2\mathbf{T}}{\partial t^2}\right|_{\mathbf{T}(t^k)} + \ldots \tag{6}$$

Here, time and space discretization is accomplished by setting $\delta t = \Delta t$, $T^k = T(t^k)$ and $T^{k+1} = T(t^k + \Delta t)$. This yields approximations for the first order derivative $\partial\mathbf{T}/\partial t$ and the second order derivative accordingly at the location with index i and j:

$$\left.\frac{\partial T_{i,j}}{\partial t}\right|_{T_{i,j}^k} \approx \frac{T_{i,j}^{k+1} - T_{i,j}^k}{\Delta t}, \quad \left.\frac{\partial^2 T}{\partial\varphi^2}\right|_{T_{i,j}^k} \approx \frac{T_{i-1,j}^k - 2T_{i,j}^k + T_{i+1,j}^k}{\Delta\varphi^2} \tag{7,8}$$

2.3. Model parameters and boundary conditions for abrasive circular cutting

The outlined approach is frequently proved for simulation of work piece temperature in grinding [23]. Fig. 1 shows the geometry of the tested tool as well as the structure of the FDM model. Temperature change of an individual element is given by:

$$\frac{T_{i,j}^{k+1}-T_{i,j}^{k}}{\Delta t}=\frac{\lambda}{\rho c}\left(\frac{T_{i,j-1}^{k}-2T_{i,j}^{k}+T_{i,j+1}^{k}}{\Delta r^{2}}+\ldots\right.$$
$$\left.\ldots+\frac{1}{j\Delta r}\frac{T_{i,j+1}^{k}-T_{i,j-1}^{k}}{2\Delta r}+\frac{1}{(j\Delta r)^{2}}\frac{T_{i-1,j}^{k}-2T_{i,j}^{k}+T_{i+1,j}^{k}}{\Delta\varphi^{2}}\right) \quad (9)$$

The time increment is set to $\Delta t = r\,\Delta\varphi / v_c$ such that the heat source moves for each time step by a spatial increment along the wheel periphery. With the feed length as sum of sample length l_s and transition $l_{transition}$ (see Fig. 1 and 2), the ambient temperature T_∞ and the feed velocity v_f the boundary conditions of the model are as follows:

$$\lambda\frac{\partial T_{i,j}^{k}}{\partial z}=-\alpha\left(T_{i,j}^{k}-T_{\infty}\right) \quad (10)$$
$$\lambda\frac{\partial T_{i,j}^{k}}{\partial r}=\begin{cases}q''_{cutting}(t) & j=1, i=i_{cz}(k), t<t_{cutting}\\ -\alpha\left(T_{i,j}^{k}-T_{\infty}\right) & other\end{cases}$$
$$T^{0}{}_{i,j}=T_{\infty}$$
$$\text{with } t_{cutting}=\left(l_S+l_{transition}\right)/v_f$$

By means of the function $i_{cz}(k)$ the angular increment being in peripheral contact with the work piece at the instant time $t = k\Delta t$ is calculated.

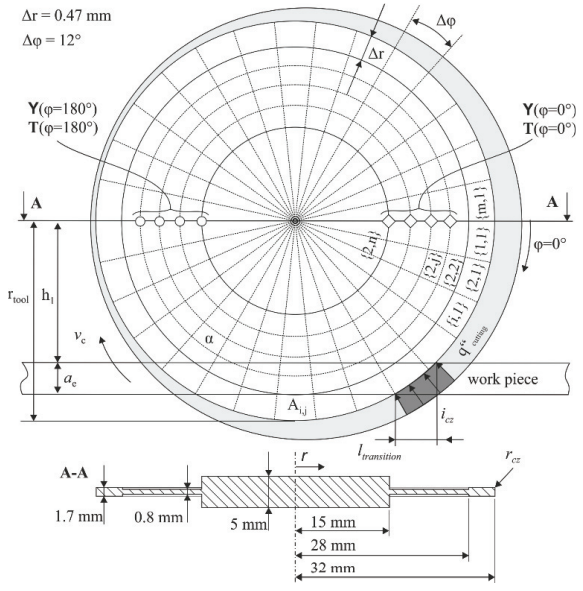

Figure 1 Tool geometry and structure of the FDM model

The function of input heat flux density $q''_{cutting}(t)$ is composed of a stationary part and a superimposed periodic part with variable amplitude. The latter accounts for a radial run-out of the tool and additional dynamic imperfections of the experimental set up.

$$q''_{cutting}(k)=\eta\cdot\frac{P_c}{A_{i,1}}\left(1+\gamma(k\Delta t)\cdot\cos(k\Delta t\Delta\varphi)\right) \quad (11)$$
$$\text{with } \gamma(k\Delta t)=\gamma_a\cdot(k\Delta t)^2+\gamma_b\cdot k\Delta t+\gamma_c$$

Furthermore, the following constant parameters are used: Specific heat capacity of the tool c_p = 0.43 J/gK, density ρ = 0.00805 g/mm³, ambient temperature T_∞ = 22 °C.

The unknown parameter vector **p** consists of coefficient η representing cutting power fraction into the tool, polynomial fitting coefficients for cutting power variation γ_a, γ_b, γ_c, heat conductivity of the tool λ [W/mK] and the heat transfer coefficient tool - air α [W/m²K]. Thus, this 2-dimensional approach firstly neglects possible heat exchange between the tool side faces and the machined slot.

3. Experimental methods

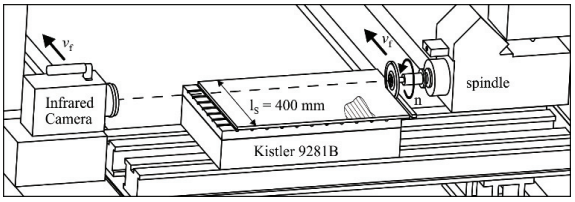

Figure 2 Experimental setup

Dry cut-off grinding tests were carried out on CFRP specimens of thickness $t = a_e$ = 4 mm and length l_S = 400 mm. Specimens were clamped by vacuum on a jig that was mounted to a force dynamo-meter. A five-axis machining center (Reichenbacher Vision) was used, Fig. 2. CFRP consists of unidirectionally laminated plies of HTS carbon fibers with a volume fraction of 60% and epoxy resin Cycom 977-2. Specimens were oriented with respect to the feed direction at Φ = 0° and 90°, respectively. The geometry of the electroplated abrasive circular cutting wheel is specified in Fig. 1. Its core (HS 6-5-2) was diamond equipped with a grain size of D427 on periphery and protruding annular face sides. Immersion depth is expressed by the ratio h_l/r_{tool} of axis height above the work piece surface h_l and tool radius r_{tool} that is set to 0.72 and 0.84 respectively, cutting speeds v_c = 30.1, 36.8 and 43.5, and feed velocities v_f = 1.5, 3.0 and 4.5 m/min were tested.

Aligned with the tool axis an infrared camera was directed to one face side which was painted in black for improved thermal emissivity. By comparison with thermocouple measurements the tool emission coefficient was determined to ε = 0.94. Temperature fields on the tool surface were recorded during cut-off grinding with a frequency of 500 Hz along the feed path and subsequent cooling time of the rotating tool.

4. Results and discussion

4.1. Evaluation of cutting power measurements

In Fig. 3 the cutting power per square millimeter slot area is shown separated by fibre orientation angle and immersion depth. The power increases linear with feed velocity v_f and is almost independent of the cutting speed v_c. Within the parameter set the measured cutting power, when cutting samples with a fibre orientation angle of Φ = 0° and a low immersion depth, is significantly the lowest. The results correspond to the findings of Hintze and Hartmann [24] that the cutting force and hence the cutting power is affected by the fibre cutting angle. Whereas the fibre cutting angle varies at a fibre orientation angle of Φ = 0° with changes of the immersion depth, the fibre cutting angle is independent at Φ = 90°. In the latter case it is always 90°.

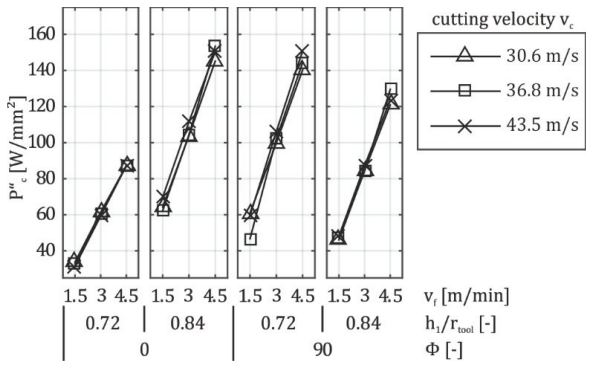

Figure 3 Measured cutting power per square millimetre slot area P''_c

4.2. Evaluation of temperature measurements and model parameter evaluation

In order to identify the parameter vector **p** of the heat flux model, simulated and measured temperatures $\mathbf{T}_l^k$ and $\mathbf{Y}_l^k$ at discrete spatial points l and time steps k are compared and the resulting error is minimized, see equation (2). For spatial referencing of simulation and measured temperatures, points are selected at angles of maximal and minimal temperature and heat flux, i.e. φ = 0° and φ = 180°, Fig. 1. Starting at a radius r_j = 28 mm 15 temperatures $\mathbf{T}_l^k$ with a radial step width Δr towards the center are captured. The frames from the infrared camera are evaluated at corresponding radii on a horizontal, radial trace.

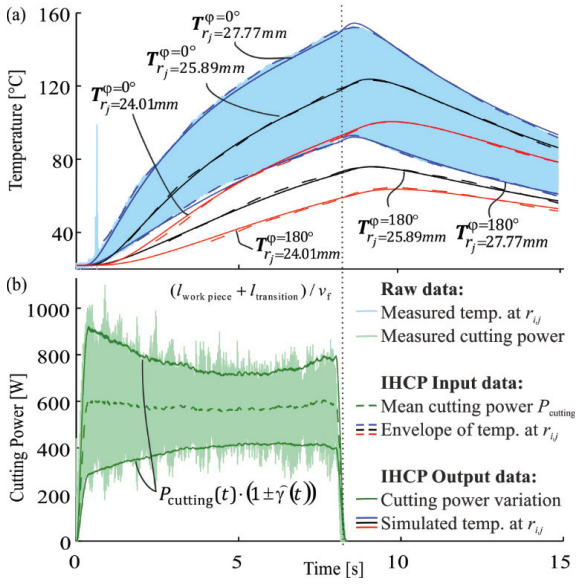

Figure 4 a) Envelopes of measured and simulated temperature profiles at radial tool positions r_j = 27.77 mm, 25.89 mm, 24.01 mm, b) measured and simulated cutting power profiles with estimated polynomial coefficients γ_a = 0.0099, γ_b = -0.109, γ_c = 0.56 with η = 0.25 for v_c = 36.9 m/s, v_f = 3.0 m/min, h_1/r_{tool} = 0.84, Φ = 90°

Due to missing synchronization of infrared frames and spindle speed each curve oscillates between minimum and maximum temperatures with the frequency of the spindle speed. For comparison with simulated temperatures $\mathbf{T}_l^k$ upper and lower envelopes are calculated for measured temperatures at each radius, which are shown for three radii in Fig 4. These envelopes account for the maximum and minimum temperatures $\mathbf{Y}_l^k$. Temperature-time-curves for certain radii show a transient increase during tool engagement and after exit of the tool from the work piece a transient decrease.

Fig. 5a shows the tool temperature field measured on a face side section of the tool indicating non-uniform temperature distribution on radially opposite sides. The left side corresponds to φ = 180°, the right side to φ = 0° in the FDM model domain, i.e. to minimum and maximum heat flux respectively.

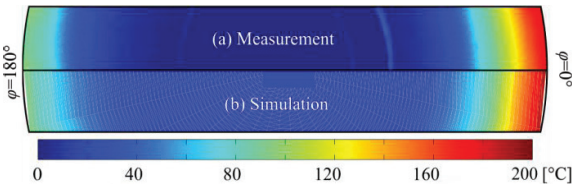

Figure 5 a) Measured, b) simulated temperature field, Φ = 0°, v_c=36.9 m/s, v_f = 3.0 m/min, h_1/r_{tool} = 0.72, t = 7,488 s, estimated model parameters λ = 24.6 W/mK, α = 130 W/m²K, η = 0.27, γ_a = -0.0025, γ_b = -0.007, γ_c = 0.52

With a first simulation run a common heat conductivity of the tool λ = 24.1 W/mK and heat transfer coefficients tool - air α are determined from the temperature profiles in the cooling phases. In accordance with physical expectation [12] an increase of α with the cutting speed v_c was found between α (v_c = 30 m/s) = 110 W/m²K and α (v_c = 43.6 m/s) = 150 W/m²K, which is reasonable compared with the results from Northrop and Owen [25]. Subsequently, the parameters λ and α are set constant and the remaining parameters η, γ_a, γ_b and γ_c are identified from the temperature profiles in the heating phases under various cutting conditions. The identified coefficients η are depicted in Fig. 6.

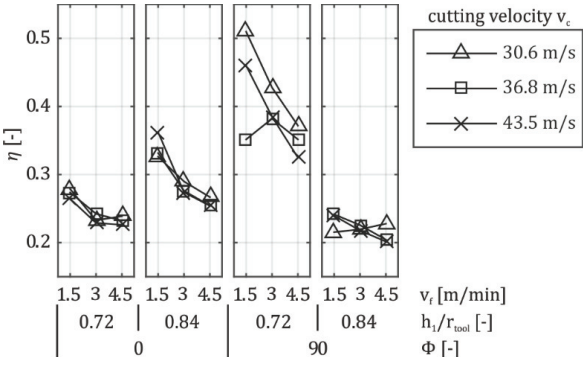

Figure 6 Estimated ratio of heat flux into the tool η

The ratio of heat flux into the tool η slightly decreases with feed velocity v_f. Irrespective of the other cutting parameters η is in a narrow interval of 0.23 < η < 0.37 for Φ = 0°. In contrast, for Φ = 90°, η is significantly influenced by the immersion depth. The coefficient η can be qualitatively substituted by a flux divider at parallel resistances R or conductivities G of tool and workpiece, accordingly [18].

$$\eta \approx \frac{R_{total}}{R_{tool}} = \frac{G_{tool}}{G_{workpiece} + G_{tool}} = \frac{1}{1 + \frac{G_{workpiece}}{G_{tool}}} \quad (12)$$

Considering the 15 times higher thermal conductivity of CFRP in fiber direction than perpendicular to it [5], the conductivity perpendicular can be neglected and thus the conductivity of the workpiece is proportional to the size of the projected contact zone in fiber direction. Due to the shape of the abrasive grains, in fact, the geometry of the real contact zone is toric with an according radius of $r_{cz} \approx 0.43$ mm. Whereas the size of projected tool segment for $\Phi = 0°$ is equal to the slot area $A = b_s \cdot a_e$ and does not change with the immersion depth, the size changes for $\Phi = 90°$. It becomes larger for increasing h_1/r_{tool} and thus η decreases.

Simulation and measurements are in good agreement, the mean error of temperatures is below 2.0°C. The simulated temperature field for one instant of time is depicted in Fig. 5b. Hence, maximum temperature at the tool periphery reaches 200°C after a cutting time $t \approx 7.5$ s. With regard to the simulated temperature-time curves in Fig. 4a the increase and dynamics of temperature profiles are well represented by the model. Based on the parameters of Fig. 4 simulation for longer cutting times leads to a maximum tool temperature of 300° C in steady state at $t \approx 60$ s. Thus, temperatures in abrasive circular cutting do not exceed those in end milling at similar feed velocities and material thickness [6, 13]. As shown in Fig. 4b, the identified polynomial fitting coefficients γ_a, γ_b, γ_c provide excellent approximation of the measured dynamic cutting power profile.

5. Summary and outlook

- A model for simulation of transient heat flux in dry abrasive circular cutting of CFRP with epoxy matrix considering heat transfer at face sides and dynamic imperfections of the tool was derived.
- Cutting power is proportional to feed velocity v_f and independent of cutting speed v_c
- Evaluated heat flux ratios into the tool η indicate that the projected contact zone in fiber direction is crucial for heat dissipation.
- Temperatures in dry abrasive circular cutting of CFRP with epoxy matrix do not exceed those in dry end milling
- In order to minimize the heat flux into the work piece a high heat flux ratio into the tool η is desirable.
- Evaluation of simulated η suggest that a small profile of the contact zone on the side faces of the tool and a low immersion depth ratio h_1/r_{Tool} are recommended.

Influence of tool wear, face side geometry, different CFRP materials and dry cooling on heat flux separation as well as limitations of the direct FDM model need further investigation.

References

[1] Teti, R., 2002, Machining of composite materials, CIRP Annals, 51/2: 611-634

[2] Colligan, K., Ramulu, M., 1999, Edge trimming of graphite/epoxy with diamond abrasive cutters, *Journal of Manufacturing Science and Engineering,* 121:647-655

[3] Soo, S.L., Shyha, I.S., Barnett, T., Aspinwall, D.K., Sim, W.-M., 2012, Grinding performance and workpiece integrity when superabrasive edge routing carbon fibre reinforced plastic (CFRP) composites, *CIRP Annals,* 61/1:295-298

[4] Sheikh-Ahmad, J. Y., 2009, *Machining of Polymer Composites*, Springer

[5] Kindler, J., 2010, *Werkstückqualität und Standzeitoptimierung von Zerspanwerkzeugen bei der Umrissbearbeitung von kohlenstofffaserverstärkten Kunststoffen*, TU Hamburg-Harburg

[6] Yashiro, T., Ogawa, T., Sasahara, H., 2013, Temperature measurement of cutting tool and machined surface layer in milling of CFRP, *Int. Journ. Machine Tools & Manufacture,* 70:63-69

[7] Arisawa, H., Akama, S., Niitani, H., 2012, High-performance cutting and grinding technology for CFRP, *Mitsubishi Heavy Industries Technical Review,* 49/3: 3-9

[8] Hintze, W., Klingelhöller, C., Langhof, O., 2015, Curved sawing of thin lightweight components, *Journal of Production Engineering Research and Developmen*t, 9/51 DOI: 10.1007/s11740-014-0587-2

[9] Yamada, Y; Sasahara, H., 2014, Free-form curves cutting using flexible circular saw, *Precision Engineering*, 38:611-616

[10] Gao, H., Ma, H.L., Bao, Y.J., Yuan, H.P., Kang, R.K., 2010, Theoretical analysis of grinding temperature field for carbon fiber reinforced plastics, *Advanced materials research*, 126-128:52-57

[11] Hintze, W., Schütte, C., Steinbach, S., 2013, Influence of the fiber cutting angle on workpiece temperature in drilling of unidirectional CFRP, Lecture Notes in Production Engineering: New Production Technologies in Aerospace Industry, *Proceedings of the 4th Machining Innovations Conference*, Springer, Hannover

[12] Cardone, G., Astarita, T., Carlomagno, G.M., 1997, Heat transfer measurements on a rotating disk, *Int. Journal of rotating machinery*, 3:1-9

[13] Hohensee, V., 1990, Infrarotthermographie – ein Verfahren zur Werkzeugtemperaturbestimmung, *Magazin Neue Werkstoffe,* 1/90:13-20

[14] Lee, D.G., Kim, P.J., 2000, Temperature rise and surface roughness of carbon fiber epoxy composites during cut-off grinding, *Journal of composite materials*, 34:2061-2080

[15] Sasahara, H., Kikuma, T., Koyasu, R., Yao, Y., 2014, Surface grinding of carbon fiber reinforced plastic (CFRP) with an internal coolant supplied through grinding wheel, *Precision Engineering,* 38:775-782

[16] Ullmann, F., 1992, *Temperaturbestimmung beim Drehen faserverstärkter Kunststoffe*, Hanser, München

[17] Weinert, K., Kempmann, C., 2004, Cutting temperatures and their effects on the machining behaviour in drilling reinforced plastic composites, *Advanced engineering materials,* 6/8:684-689

[18] Tönshoff, H.K., Denkena, B., 2004, *Spanen*, Springer, Berlin

[19] Orlande, H.R.B., 2012, Inverse Problems in Heat Transfer: New Trends on Solution Methodologies and Applications, *Journal of Heat Transfer,* 134:1-13

[20] Necati Özişik, M., 2000, *Inverse heat transfer: fundamentals and applications*, CRC Press

[21] Marquardt, D.W., 1963, An Algorithm for Least-Squares Estimation of Nonlinear Parameters, *Journal of Society for Industrial and Applied Mathematics,* 11/22:431-441

[22] Hahn, D.W.; Necati Özişik, M., 2012, *Heat Conduction Hoboken*, NJ, USA: John Wiley & Sons, Inc.

[23] Brinksmeier, E., Aurich, J.C., Govekar, E., Heinzel, C., Hoffmeister, H.-W., Klocke, F., Peters, J., Rentsch, R., Stephenson, D.J., Uhlmann, E., Weinert, K., Wittmann, M., 2006 Advances in Modeling and Simulation of Grinding Processes, *CIRP Annals*, 55/2:667-696

[24] Hintze, W., Hartmann, D., 2013, Modeling of delamination during milling of unidirectional CFRP in: *Procedia of the 14th CIRP Conference on Modeling of Machining Operations* (CIRP CMMO 2013), Juni 13 - 14, 2013, Turin, Italien, Elsevier, 8: 443-448

[25] North, A., Owen, J.M., 1988, *Heat transfer measurements in rotating-disc systems part 1: The free disc*, International journal of heat and fluid flow 9/ 1:19-26